

Cloning and Immunolocalization of a Rat Pancreatic Na⁺ Bicarbonate Cotransporter

Frank Thévenod,^{*,1} Eleni Roussa,[†] Bernhard M. Schmitt,[‡] and Michael F. Romero^{§,1,1}

^{*}Department of Physiology and [†]Department of Anatomy, Medical Faculty, University of Saarland, 66421 Homburg, Federal Republic of Germany; [‡]Department of Cellular & Molecular Physiology, Yale University, School of Medicine, New Haven, Connecticut 06520; and [§]Department of Physiology & Biophysics and ¹Department of Pharmacology, Case Western Reserve University School of Medicine, Cleveland, Ohio 44106-4790

Received September 9, 1999

In the rat, pancreatic HCO₃⁻ secretion is believed to be mediated by duct cells with an apical Cl⁻/HCO₃⁻ exchanger acting in parallel with a cAMP-activated Cl⁻ channel and protons being extruded through a basolateral Na⁺/H⁺ exchanger. However, this may not be the only mechanism for HCO₃⁻ secretion by the rat pancreas. Recently, several members of electrogenic Na⁺/HCO₃⁻ cotransporters (NBC) have been cloned. Here we report the cloning of a NBC from rat pancreas (rpNBC). This rpNBC is 99% identical to the longer, more common form of NBC [pNBC; 1079 amino acids (aa); 122 kDa in human heart, pancreas, prostate, and a minor clone in kidney]. The longer NBC isoforms are identical to the rat and human kidney-specific forms (kNBC; 1035 aa; 116 kDa) at the ~980 C-terminal aa's and are unique (with different lengths) at the initial N-terminus. Using polyclonal antibodies to the common N- and C-termini of rat kidney NBC, a ~130-kDa protein band was labeled by immunoblotting of rat pancreas homogenate and was enriched in the plasma membrane fraction. Immunofluorescence and immunoperoxidase light microscopy of rat pancreatic tissue with both antibodies revealed basolateral labeling of acinar cells. Labeling of both apical and basolateral membranes was found in centroacinar cells, intra- and extralobular duct, and main duct cells. The specificity of the antibody labeling was confirmed by antibody preabsorption experiments with the fusion protein used for immunization. The data suggest that rpNBC likely plays a more important role in the transport of HCO₃⁻ by rat pancreatic acinar and duct cells than previously believed. © 1999 Academic Press

Key Words: HCO₃⁻ transport; homology cloning; secretion; ducts; acini.

Electrolyte and fluid secretion by the rat exocrine pancreas results from the sequential operation of two secretory epithelia, the secretory end pieces (acini) and the duct system (1). Following hormonal stimulation, a plasma-like primary fluid secreted by the acini is modified by the duct cells. In the rat, the secretagogue cholecystokinin (CCK) mainly acts on acinar cells by activating IP₃-, DAG-, and Ca²⁺-dependent signaling pathways and evokes an increase of the pancreatic secretory rate without alteration of the ionic composition of the final fluid; secretin stimulation, however, by increasing cAMP levels in duct cells, evokes an increase in fluid secretion rate that is associated with an increase in HCO₃⁻ concentration (to about 70 mmol/l) and a corresponding fall in Cl⁻ concentration (2).

The current model to account for ion and fluid secretion by rat pancreatic acini is based on Na⁺-coupled secondary active Cl⁻ transport (3). The cellular Na⁺ gradient generated by the basolateral Na⁺/K⁺-ATPase energizes a basolateral Na⁺/H⁺ exchanger. This process raises the cytosolic pH and promotes formation of HCO₃⁻ by hydration of CO₂, catalyzed by carbonic anhydrase. The HCO₃⁻ so formed exits to the interstitium in exchange for Cl⁻ via a Cl⁻/HCO₃⁻ exchanger in the basolateral membrane. By these means, Cl⁻ accumulates into the cell above its electrochemical equilibrium. Following stimulation by CCK, Cl⁻ exits the cell via Ca²⁺ sensitive Cl⁻ channels in the luminal membrane, and Na⁺ enters the lumen paracellularly to preserve electroneutrality (4). This basic model of acinar secretion has been subsequently modified to account for the presence of a nonselective cation conductance in the basolateral membrane that would

¹ To whom correspondence may be addressed: (F.T.) Department of Physiology, University of Saarland, Building 58, D-66421 Homburg/Saar, FRG. Fax: +49 6841 16-6655. E-mail: frank.thevenod@med-rz.uni-sb.de. (M.F.R.) Department of Physiology & Biophysics, Case Western Reserve University, School of Medicine, 2119 Abington Rd., Cleveland, OH 44106-4790. Fax: +1 216 368-3952. E-mail: mfr2@po.cwru.edu.

otherwise impede Na^+ -coupled secondary active Cl^- transport by depolarizing the cell potential (5, 6).

The prevailing model for rat ductal HCO_3^- secretion is based on studies in intralobular ducts (7, 8). In this model, HCO_3^- secretion depends on the luminal Cl^- concentration. As in pancreatic acini, HCO_3^- is generated in the cytosol by a process involving basolateral Na^+/H^+ exchanger, Na^+/K^+ -ATPase and cytosolic carbonic anhydrase. HCO_3^- enters the lumen via a luminal $\text{Cl}^-/\text{HCO}_3^-$ exchanger, the activity of which depends on a supply of luminal Cl^- delivered to it from the cytosol by a recycling process utilizing an apical cAMP-activated Cl^- channel, presumably CFTR (9). Na^+ enters the lumen across cation-permeable intercellular junctions, driven by the lumen negativity.

In both models of secretion, a crucial step involves HCO_3^- being transported out of the cell in exchange for intracellular Cl^- via a coupled $\text{Cl}^-/\text{HCO}_3^-$ exchanger, possibly from the band 3-related family of anion exchangers AE1-AE3 (10–12). The exchanger belongs to a family of HCO_3^- transporters (13), which also includes $\text{Na}^+/\text{HCO}_3^-$ cotransporters with as many as three different stoichiometries, a $\text{K}^+/\text{HCO}_3^-$ cotransporter, and a Na^+ -driven $\text{Cl}^-/\text{HCO}_3^-$ exchanger. Recently, Romero *et al.* have cloned a renal electrogenic $\text{Na}^+/\text{HCO}_3^-$ cotransport protein (NBC) from salamander and rat kidney (14, 15). Subsequently, a different form of this $\text{Na}^+/\text{HCO}_3^-$ cotransporter has been cloned from human pancreas (hpNBC) (16) and human heart (hhNBC) (17). *In situ* hybridization studies in the mouse revealed expression of pNBC in duct and acinar cells (16). The human pancreatic respective cardiac NBC form is longer (1079 amino acids (aa); 122 kDa) and has an alternative N-terminus (MEDE start) compared to the kidney specific NBC form (1035 aa; 116 kDa; MSTE at the N-terminus). Meanwhile, additional members of the NBC protein family have been cloned from human retina (NBC2) (18) and skeletal muscle (NBC3) (19). Here we report the cloning of a NBC from rat pancreas (rpNBC). This rpNBC is 99% identical to the longer, more common form of NBC from human heart and pancreas (16, 17). Using polyclonal antibodies to the common N- and C-termini of NBC (20), immunoblotting of a plasma membrane fraction from rat pancreas revealed a ~130-kDa protein band. Immunohistochemistry of rat pancreatic tissue with both antibodies revealed basolateral labeling of acinar cells. Labeling of both apical and basolateral membranes was found in intercalated, intralobular and main duct cells. The data suggest that NBC may contribute to both acinar and ductal HCO_3^- transport by the rat exocrine pancreas.

METHODS

Cloning of Rat Pancreatic NBC cDNA

Reverse transcriptase-PCR. We purchased rat pancreas poly(A)+ RNA from Clontech (Palo Alto, CA). Five hundred nanograms of RNA was heated to 70°C for 2 min and then “quick-chilled” on ice for 60 s. In a 20- μl reaction, we added an oligo-dT primer, dNTPs, and SuperScript II reverse transcriptase (Gibco-BRL, Gaithersburg, MD). The extension proceeded at 45°C for 1 h.

PCR and subcloning. We used 0.5 μl of the RT reaction for a standard 50 μl PCR using NBC gene specific primers. Since there are 2 known isoforms of NBC which vary only at the NH_2 -terminus, we PCRd between the 2 known starts (MEDE_f = 5'-ATg-gAg-gAT-gAA-gCT-gTC-CTg-gAC-AgA-ggg-3' and MSTE_f = 5'-ATg-TCC-ACT-gAA-AAT-gTg-gAA-ggg-AAg-CCC-3') and the common COOH-terminus (ERHT_r = 5'-TTA-TCA-gCA-TgA-TgT-gTg-gCg-TTC-3') in separate reactions. To assure fidelity we performed PCR using TaKaRa-ExTaq (Panvera, Milwaukee, WI). The PCR protocol was: (a) 1 cycle of 2 min 94°C, 2 min 60°C, 2 min 68°C; (b) 30 cycles of 20 s 94°C, 20 s 60°C, 3 min 68°C; then (c) final extension of 10 min 68°C. Five to eight microliters of the PCR-products was electrophoresed on an ethidium bromide 0.65% agarose gel and UV visualized. Only the MEDE_f/ERHT_r reaction yielded a product. This PCR product was directly subcloned into a TA-cloning vector, pCR2.1-TOPO, using the manufacturer's instructions (Invitrogen, Palo Alto, CA).

Sequencing. Sequencing was performed at the W. M. Keck Biotechnology Sequencing laboratory (New Haven, CT). Sequences were assembled and analyzed using the DNASTar program (Lasergene, Madison, WI) as previously reported (14). The sequence of rat pancreas NBC or rpNBC is GenBank Accession No. A107265.

Antibodies

The monoclonal antibody to the $\alpha 1$ -subunit of Na^+/K^+ -ATPase (purified rabbit kidney Na^+/K^+ -ATPase) was obtained from Upstate Biotechnology (Hamburg, Germany). Generation and specificity of the rabbit polyclonal antisera anti-(MBP-NBC-3) serum raised against rat kidney NBC (rkNBC) NH_2 -terminal amino acids 338–391 and anti-(MBP-NBC-5) serum raised against rkNBC COOH-terminal amino acids 928–1035 have been established elsewhere (20). Both antisera and the respective antigens (fusion proteins MBP (“maltose binding protein”)-NBC-3 or MBP-NBC-5) were generously provided by Dr. Walter F. Boron (Department of Cellular and Molecular Physiology, Yale University School of Medicine, New Haven, CT; supported by NIH Grant DK30344).

Preparation of Subcellular Fractions of Rat Pancreatic Tissue, SDS-PAGE, and Immunoblotting

Pancreas from 4–6 male Wistar rats (180–250 g; Charles River GmbH, Sulzfeld, Germany) fasted overnight were quickly removed into ice-cold homogenization buffer (in mM): 280 mannitol, 10 KCl, 1 MgCl_2 , 0.2 Pefabloc SC, 10 Hepes, pH 7.0 adjusted with Tris. Glandular tissue was minced into a fine paste and homogenized by 7 strokes at 500 rpm with a motor-driven glass-in-Teflon Potter-Elvehjem homogenizer. The crude homogenate was further disrupted by nitrogen pressure cavitation (750 psi for 1 min). All subsequent fractionation steps were performed using a combination of differential and discontinuous sucrose gradient centrifugation procedures described in details elsewhere (21). Purity of the plasma membrane fraction was determined in three different membrane preparations by immunoblot analysis of the $\alpha 1$ -subunit of Na^+/K^+ -ATPase (see below).

Rat pancreatic tissue homogenate and plasma membrane fractions

were heated to 37°C for 30 min in sample buffer, separated by SDS-PAGE on 7.5% acrylamide minigels and blotted onto PVDF membranes, essentially as described earlier (22). After blocking with Tris-buffered saline containing 0.1% Tween 20 and 3% milk, the membranes were incubated with primary antibodies (mouse monoclonal to the $\alpha 1$ -subunit of Na^+/K^+ -ATPase (0.1 $\mu\text{g}/\text{ml}$), rabbit anti-(MBP-NBC-3) or anti-(MBP-NBC-5) sera (1:1000) overnight followed by horseradish peroxidase-conjugated secondary antibodies (1:10,000) (sheep anti-mouse and donkey anti-rabbit IgG purchased from Amersham-Buchler, Braunschweig, FRG) for 1 h. The blots were developed with ECL reagent (Amersham, Braunschweig, Germany), and signals were visualized on X-ray films. X-ray films were scanned with a single pass flat-bed scanner (Linotype-Hell, Eschborn, FRG) and processed for documentation using a JASC Paint Shop Pro 4.1 software (Jamein, FRG). For antibody-pre-absorption experiments, primary antibodies were preabsorbed at ~22°C for 1 h with 10 $\mu\text{g}/\text{ml}$ of one of the fusion proteins MBP-NBC-3 or MBP-NBC-5.

Tissue Preparation for Immunohistochemistry

Male Wistar rats (200 g) were anesthetized with pentobarbital (Nembutal) (65 mg/kg body wt, intraperitoneally) and perfusion-fixed with 2% paraformaldehyde/75 mM lysine/10 mM sodium periodate (PLP), as described by McLean and Nakane (23). Pancreas were quickly removed, cut into pieces and additionally fixed by immersion in fresh PLP fixative overnight at 4°C. PLP-fixed tissue was washed 4 times for 10 min with phosphate-buffered saline (PBS) and kept in PBS containing 0.02% sodium azide at 4°C until further use.

Immunofluorescence and Immunoperoxidase

Light Microscopy

Tissue blocks were cryoprotected in 30% sucrose for at least 1 h, frozen in liquid N_2 and cut in 5- μm cryosections. Indirect immunofluorescence was performed as described by Alper *et al.* (24) with minor modifications. Cryosections were rehydrated in PBS for 5 min and incubated with 1% SDS for 5 min to enhance antigen retrieval (25). After three 5-min washes with PBS, sections were treated with PBS containing 1% BSA for 15 min to reduce background staining and subsequently incubated with the primary antibody diluted 1:600 to 1:800 in PBS containing 0.02% sodium azide for 2 h at room temperature (RT). Sections were washed 3 times for 5 min in PBS, incubated with donkey anti-rabbit IgG coupled to indocarbocyanin (CY3) (1:600 dilution) (Amersham-Buchler, Braunschweig, FRG) for 1 h at RT, washed 3 times for 5 min with PBS and mounted with Vectashield (Vector Laboratories, Linaris, Bettingen, FRG) diluted 2:1 in 0.1 M Tris-HCl (pH 8.0). Labeled sections were examined using an Olympus BX50F microscope equipped with a 40 \times Olympus UPlanFI objective and a narrow band green fluorescence exciter filter (λ 530–550 nm). Images were recorded with a 3CCD color video camera (Sony DXC-950) and were digitized to 8 bits/pixel using a software developed in the laboratory. Digitized images were processed for documentation using an Adobe Photoshop D1-4.0 software (Herzogenaurach, FRG).

For immunoperoxidase light microscopy, sections were initially treated as described above. After incubation with the primary antibody, sections were washed 3 times for 5 min in PBS, incubated with biotinylated goat anti rabbit IgG (1:100 dilution) for 1 h at RT, washed 3 times for 5 min with PBS and incubated with Vectastain ABC reagent (Vector Laboratories, Linaris, Bettingen, FRG) for 1 h at RT. Sections were then washed 3 times for 5 min with PBS and peroxidase reaction was visualized by development in DAB-hydrogen peroxide substrate medium. Sections were dehydrated in a graded series of ethanol concentrations, cleared in xylene and mounted with DePeX. Labeled sections were examined with a light microscope (Olympus; Tokyo, Japan). Images were recorded with charge-coupled

device cameras connected to a frame grabber that was mounted in an IBM-compatible personal computer. To increase sharpness, digitized images from three adjacent optical planes were merged in Adobe Photoshop D1-4.0.

Control experiments were performed by either omitting the primary antibody or incubating the sections with the primary antibody in the presence of 10 $\mu\text{g}/\text{ml}$ fusion protein antigen.

RESULTS

Cloning of rNBC

Here we report the cloning of a NBC from rat pancreas (rpNBC). Figure 1 illustrates that rpNBC is 99% identical to NBC recently reported in human pancreas (16) and human heart (17). This NBC clone initiates with the sequence "MEDE . . .," encodes 1079 amino acids (aa) and predicts a protein of 122 kDa. NBC from both the rat (15) and human (26) kidney possess a start sequence of "MSTE . . .," are 1035 aa and predict 116-kDa proteins. In humans, the "MSTE" clone-start appears to be kidney specific while the "MEDE" clone-start seems the more common NBC form (13, 16). Indeed, using the same RT-PCR protocol, we were not able to amplify the MSTE full-length clone, i.e., rkNBC, from rat pancreas. Figure 1 also shows that the two forms differ only at the NH_2 -terminus in both human and rat.

Due to the high identity, this rpNBC clone shares most of the predicted structural features with rkNBC (15), but also contains the additional putative sites and features found in human pancreas and heart (16, 17). rpNBC has both the NH_2 - and COOH -termini cytosolic, a minimum of ten transmembrane spans (TMs), and a large extracellular loop connecting TM5 and TM6. This 5,6-loop contains 4 predicted N-linked glycosylation sites. The alternative NH_2 -terminus of rpNBC has a putative phosphorylation site for protein kinase A (PKA) at T49, an additional PKA site is also present at the COOH -terminal end (S1026). The clone has multiple consensus protein kinase C (PKC) phosphorylation sites, two of them are found in the alternative NH_2 -terminus (S38, S65). There is also one predicted tyrosine phosphorylation site (Y941). Two DIDS-binding motifs (K-(Y) (X)-K, where Y = M, L and X = I, V, Y) are additional characteristic "signature" sequences of the NBC proteins. The sequence KMIK can be found in the extracellular loop connecting TM5 and TM6 (aa 603–606) and the motif KLKK in the extracellular loop between TM7 and TM8 (aa 812–815). Table 1 highlights all the putative modification sites of rpNBC.

Immunoblotting of Rat Pancreas

To identify the NBC protein in rat pancreas, we performed immunoblotting experiments with rabbit anti-(MBP-NBC3) and anti-(MBP-NBC5) antisera, whose characterization and specificity has been previ-

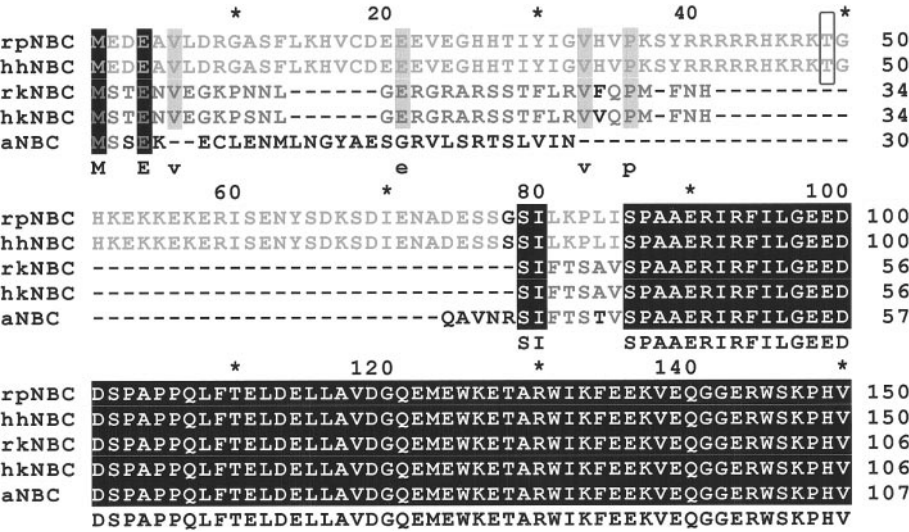


FIG. 1. Sequence alignment of the known NBC variants to date and *Ambystoma tigrinum* kidney form of NBC (aNBC). The mammalian forms of NBC segregate into two groups: clones initiating with the sequence “MEDE . . .” and clones initiating with the sequence “MSTE . . .”. Interestingly, the originally cloned *Ambystoma tigrinum* kidney form of NBC (aNBC) appears to be equidistant from both sets of clones (13). Illustrated here are the two starts as well as the beginning of the common and identical NH₂-termini. The second predicted PKA site (T49) is denoted by a frame. In the last line of the alignment, highly conserved amino acids (aa) are indicated by capital letters, and aa found in mammalian NBC forms, but not in aNBC, are represented by lowercase letters.

ously described (20), on homogenate from whole rat pancreas and the plasma membrane fraction. The purity of the plasma membrane fraction was ascertained by immunoblotting with a monoclonal antibody to the α 1-subunit of Na⁺/K⁺-ATPase (0.1 μ g/ml) (Fig. 2). An enrichment factor of 14.4 ± 3.2 was determined in the plasma membrane fraction (PM) for the α 1-subunit of Na⁺/K⁺-ATPase, compared to pancreas homogenate (Ho). As shown in Fig. 2 (lanes “–antigen”), both anti-(MBP-NBC3) and anti-(MBP-NBC5) antisera detected a prominent band of ~130 kDa in the plasma membrane fraction, whereas this band was not detectable in pancreatic tissue homogenate. This molecular weight approximates that of 122 kDa predicted from the cDNA

sequence of rat pancreatic NBC and is also similar to the major immunoreactive band identified as NBC protein in rat kidney microsomes (20). The specificity of the labeling of the ~130-kDa band observed in the plasma membrane fraction of rat pancreas was tested by preincubation with an excess (10 μ g/ml) of the respective antigens. Labeling of the ~130 kDa band by the antisera was prevented (Fig. 2, lanes “+antigen”), indicating that the ~130-kDa band labeled by the antisera is specific for rat pancreatic NBC.

The anti-(MBP-NBC3) antiserum also routinely detected a minor band at ~50 kDa, whereas the anti-(MBP-NBC5) antiserum labeled a band at ~100 kDa. Labeling of both bands was abolished by pre-

TABLE 1
Putative Modification Sites of rpNBC

Predicted type	Consensus site	Sites (rpNBC)
N-linked glycosylation	N-{P}-[ST]-{P}	541, 636, 641, 661
PKA	[RK](2)-x-[ST].	T49, S1026
PKC	[ST]-x-[RK]	S38, S65, T128, T216, T249, S262, S400, T439, T750, S854, S1039, S1044, S1064
Casein kinase II	[ST]-x(2)-[DE]	S68, T110, S157, T163, S223, S239, S257, S336, S408, T419, S995, S1000, S1029, S1064, T1071
Tyrosine phosphorylation	[RK]-x(2,3)-[DE]-x(2,3)-Y	Y941
Myristylation	G-{EDRKHPFYW}-x(2)-[STA GCN]-{P}	G423, G427, G488, G500, G507, G512, G520, G558, G679, G683, G702, G1025

Note. For further details, see text. “[]” indicates that one of the listed amino acids is present, and “{ }” indicates that an optional amino acid may be present.

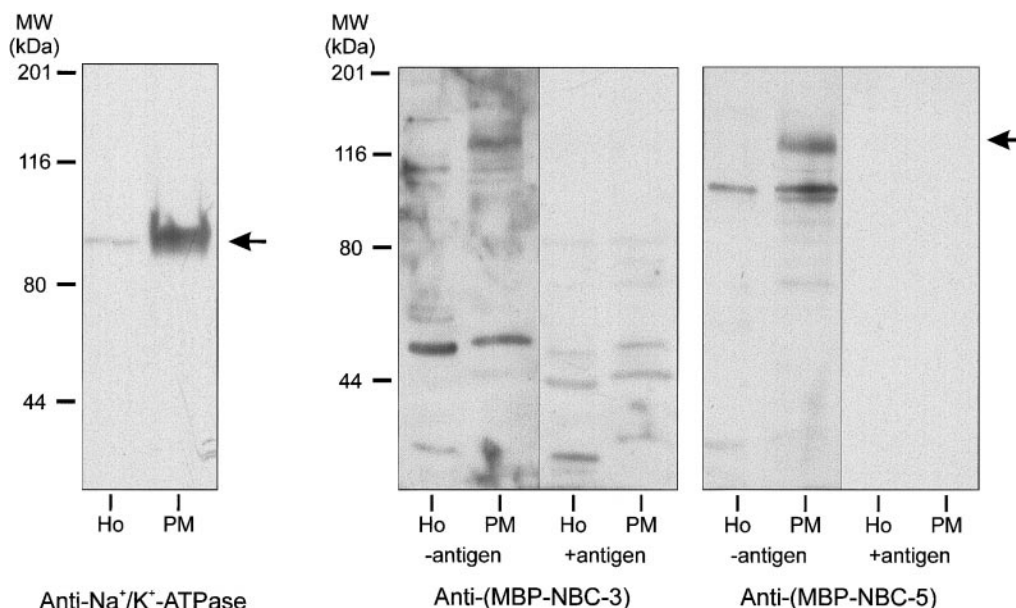


FIG. 2. Immunoblotting of rpNBC in rat pancreas. The immunoblots were either probed with a monoclonal antibody to the $\alpha 1$ -subunit of Na^+/K^+ -ATPase (0.1 $\mu\text{g}/\text{ml}$), rabbit polyclonal antiserum (anti-(MBP-NBC-3); 1:1,000) raised against rat kidney NBC (rkNBC) NH_2 -terminal amino acids 338–391 fusion protein or anti-(MBP-NBC-5) serum (1:1,000) raised against rkNBC COOH-terminal amino acids 928–1035 fusion protein (20). The specificity of labeling was tested by pre-absorption of the antisera with their respective fusion protein antigens (10 $\mu\text{g}/\text{ml}$) (“+antigen”). The blot is typical for three different membrane preparations.

absorption of the antisera with an excess concentration (10 $\mu\text{g}/\text{ml}$) of the respective antigens, suggesting that these two bands have NBC-specific epitopes.

NBC Distribution in Rat Pancreas

NBC localization in rat pancreas was examined using immunoperoxidase immunofluorescence light microscopy with antibodies raised against rat kidney NBC (rkNBC) NH_2 -terminal amino acids 338–391 (anti-(MBP-NBC-3)), or rkNBC COOH-terminal amino acids 928–1035 (anti-(MBP-NBC-5)). Both antibodies gave identical immunostaining. However, application of an epitope unmasking protocol, by treating the sections with 1% SDS for 5 min prior to antibody incubation, considerably enhanced immunolabeling intensity (25).

Figure 3 (“–antigen,” left) shows the acinar labeling pattern in cryosections of PLP-fixed rat pancreas with the anti-(MBP-NBC-5) antibody. These results were confirmed in four different animals. Similar results were obtained with the anti-(MBP-NBC-3) antibody (data not shown). Acinar staining appeared sharp and clearly localized at the basolateral cell side of moderate to strong intensity, representing NBC expression at the basolateral plasma membrane. Only rarely did single acinar cells show an apical (Fig. 3, asterisks) or granular (Fig. 3, arrowheads) staining. Labeling pattern of acini was identical with both immunoperoxidase and immunofluorescence procedures (not shown). Immunofluorescence labeling of intralobular pancre-

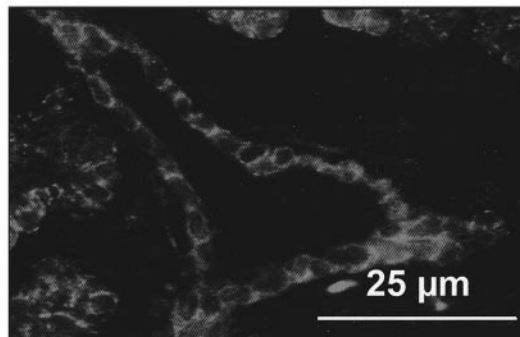
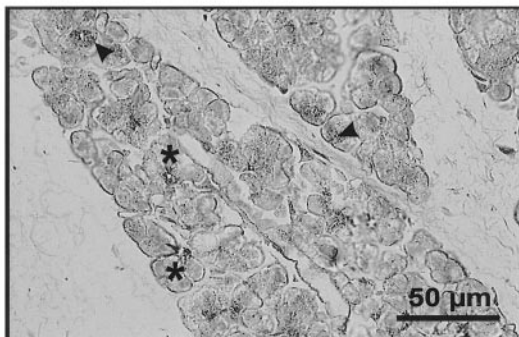
atic duct cells with the anti-(MBP-NBC-3) antibody is shown in Fig. 3 (“–antigen,” right). Intralobular, but also interlobular and main duct cells (not shown) were labeled on both, apical and basolateral cell sides by both, anti-(MBP-NBC-3) and anti-(MBP-NBC-5) antisera (not shown). However, staining did not appear uniform within the cells lining the ducts. Some cells showed apical staining, whereas basolateral staining was observed in other cells. Again, labeling of ducts was identical with both, immunofluorescence and immunoperoxidase procedures (not shown). Both, acinar and duct cell labeling (“+antigen”) were abolished in pre-absorption experiments with 10 $\mu\text{g}/\text{ml}$ fusion protein antigen.

Although NBC immunostaining of duct cells by immunofluorescence and immunoperoxidase was strong and highly reproducible, acinar cell labeling was not consistent in the eight animals studied. In two animals, acinar labeling was not restricted to the basolateral membrane, but diffusely distributed at the basolateral cell side. Moreover, in two animals no acinar NBC immunoreactivity was detected at all. Thus, it is possible that high proteolytic activity of acinar cells may destroy the cytosolic NBC epitopes during the fixation process. This indicates that acinar cells are more sensitive to fixation and tissue processing for immunohistochemistry than duct cells. Consequently, results should be more susceptible to experimental variability.

Acini

Ducts

-antigen



+antigen

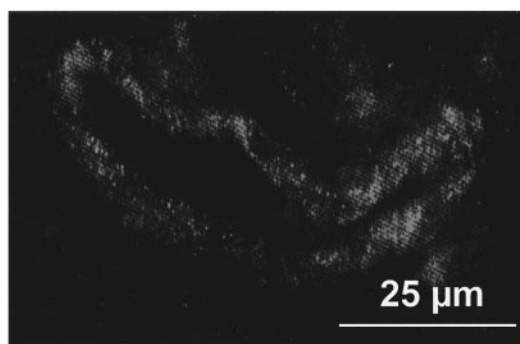
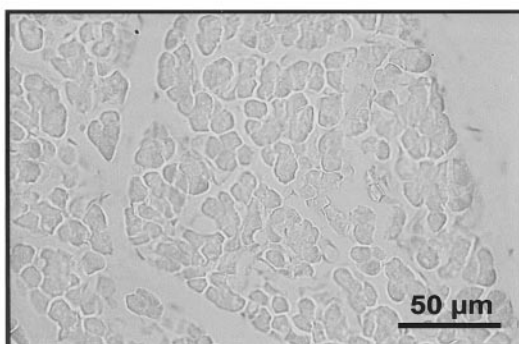


FIG. 3. Immunolocalization of rpNBC using immunoperoxidase (left) and immunofluorescence light microscopy (right). Acinar cells (left; “-antigen”) showed pronounced NBC immunolabeling with the anti-(MBP-NBC-5) antibody (dilution 1:600) at the basolateral cell side. Cells showing apical labeling are indicated by asterisks and arrowheads point to cells with granular NBC distribution. Identical staining pattern was obtained with the anti-(MBP-NBC-3) antibody (not shown). Pancreatic duct cells (right; “-antigen”) showed a complex distribution pattern: cells displayed apical and basolateral NBC staining (dilution of anti-(MBP-NBC-3) 1:600) as well as apical or basolateral labeling only. The same staining pattern was found with the anti-(MBP-NBC-5) antibody (not shown). This variability was observed in different duct segments and also within the same duct. Absence of staining upon pre-incubation of the antibody with 10 µg/ml fusion protein antigen (“+antigen”) demonstrated the specificity of the antibody.

DISCUSSION

The results of the present study demonstrate that NBC is expressed in rat exocrine pancreas, both at the mRNA and protein level. Compared to the kidney-specific form kNBC (1039 aa, “MSTE . . .”), this alternative form is longer and has a different NH₂-terminus (1079 aa, “MEDE . . .”). One distinguishing characteristic of the human NBC genes are the NBC clone starting amino acids, “MEDE” vs “MSTE.” kNBC (MSTE-start), originally expression cloned from the kidney of the salamander *Ambystoma tigrinum* (14), seems to be exclusive to the kidney of both rats and humans. In contrast, the other NBC form (MEDE-start) appears to be the more generic form of NBC and is found as a minor component also in the human kidney (13, 27). There are some obvious differences between the two NBC forms: length of NH₂-terminus, additional PKA site, and several additional PKC sites. Nevertheless, the human NBC forms appear functionally very similar (electrogenic, Na⁺-dependent, HCO₃⁻-dependent,

Cl⁻ independent, and blockable by DIDS) when expressed in *Xenopus* oocytes (17). Thus, future studies will be crucial to determine if there are differences in these two NBC proteins: regulation by second messengers, intracellular sorting, and changes in apparent ionic affinities.

Abuladze *et al.* (16) found by *in situ* hybridization that NBC is expressed in acinar and duct cells of mouse pancreas. The present data however prove that NBC is expressed in rat pancreas at the protein level. The immunoblotting experiments of our study demonstrate expression of an immunoreactive protein of ~130 kDa (the approximate molecular weight of rpNBC) in a plasma membrane fraction (Fig. 2). Additional immunoreactive bands are also detected at about 50 kDa (antibody MBP-NBC-3) and 100 kDa (antibody MBP-NBC-5). They could either represent proteolytic fragments of rpNBC (e.g., a 50-kDa NH₂-terminal fragment labeled by the anti-(MBP-NBC3) antiserum and a 100 kDa COOH-terminal fragment recognized by the

anti-(MBP-NBC5) antiserum) or different NBC-forms. The exact nature of these two additional immunoreactive bands however remains to be determined.

Immunolocalization of rpNBC was ascertained by two different techniques: immunoperoxidase and immunofluorescence. Both methods show the same distribution of NBC in exocrine pancreas, with a predominant localization in the plasma membrane of acinar and duct cells, which is in accordance with the western blot data. In acinar cells, localization of NBC is mostly basolateral (Fig. 3; "–antigen" left). Using pH measurements with the fluorescent dye BCECF, Muallem and Loessberg (28, 29) have demonstrated $\text{Na}^+/\text{HCO}_3^-$ cotransport in the basolateral membrane of rat pancreatic acinar cells that may partially account for the HCO_3^- -dependent component of acinar secretion. Using a thermodynamic approach the authors concluded from experimental manipulations of intracellular pH that the $\text{Na}^+/\text{HCO}_3^-$ cotransporter of rat pancreatic acinar cells operates with a 3:1 stoichiometry and is responsible for HCO_3^- efflux under basal conditions. Interestingly, the secretagogue cholecystokinin, which depolarizes the cell and increases cytosolic $[\text{Ca}^{2+}]$, reduced the rate of $\text{Na}^+/\text{HCO}_3^-$ cotransport and reversed the direction of transport to HCO_3^- influx (29). However, these studies rely on pH measurements only, compared to the criteria outlined by Boron and Boulpaep for identification of electrogenic $\text{Na}^+/\text{HCO}_3^-$ cotransport, i.e., Na^+ - and HCO_3^- -dependent, Cl^- -independent, DIDS-sensitive simultaneous changes of intracellular pH and membrane voltage (30). Nevertheless, they open a door to some speculation on the possible physiological significance of a basolateral $\text{Na}^+/\text{HCO}_3^-$ cotransporter in rat pancreatic acinar cells for salt and fluid secretion. It is possible that during Ca^{2+} -dependent secretagogue stimulation rpNBC may contribute to HCO_3^- influx, resulting—by parallel operation with a basolaterally located $\text{Cl}^-/\text{HCO}_3^-$ exchanger (E. Roussa, S. L. Alper, and F. Thévenod, *in preparation*)—in Cl^- accumulation into the cell ("pull-phase" of the "push-pull" model of Cl^- secretion) (5, 6).

Immunolocalization of rpNBC in duct cells was highly reproducible and had a strong staining pattern (Fig. 3, "–antigen"). Immunolabeling within one given pancreatic duct however varied between cells, some cells showing luminal and basolateral labeling, as well as labeling being restricted in other cells to the luminal or basolateral membrane areas. Whereas cellular heterogeneity of H^+ - and HCO_3^- -transporters is well documented in rat kidney collecting duct (31, 32) and salivary glands (33, 34), to our knowledge such findings have not been reported in pancreatic ducts so far. It can well be that in pancreatic duct cells the localization of transporters may differ depending on their functional state, as has been reported for vacuolar-type H^+ -ATPase for agonist evoked stimulation (35, 36). A

basolateral localization of a $\text{Na}^+/\text{HCO}_3^-$ cotransporter in intralobular and main segments of rat exocrine pancreas has been proposed by Zhao *et al.* (37) based on pH measurements with BCECF. These observations have been recently extended by Ishiguro *et al.* (38), who measured intracellular pH and Na^+ in guinea-pig interlobular ducts with the fluorescent dyes BCECF and SBFI, respectively. These results challenge the current model of agonist-induced HCO_3^- secretion developed in the rat pancreatic duct by demonstrating that a basolateral $\text{Na}^+/\text{HCO}_3^-$ cotransporter may contribute up to 75% of $\text{Na}^+/\text{HCO}_3^-$ taken up by guinea pig pancreatic duct cells during stimulation with secretin (38). The basolaterally localized rpNBC could be responsible for cellular HCO_3^- supply of the duct cell from the blood during secretin stimulated HCO_3^- secretion. This is further supported by a current report (39), in which cAMP-stimulation of a $\text{Na}^+/\text{HCO}_3^-$ cotransporter was found only in duct cells expressing functional CFTR. The link between luminal Cl^- secretion and basolateral Na^+ -dependent HCO_3^- influx was attributed to the respective changes in membrane voltage (39).

In summary, the expression of NBC in rat exocrine pancreas, its basolateral localization in acinar cells, and its distribution in both, apical and basolateral membranes of duct cells suggest a more important role for the $\text{Na}^+/\text{HCO}_3^-$ cotransporter in acid-base homeostasis of rat pancreatic acinar and duct cells and possibly a reevaluation of standard models of HCO_3^- secretion by the rat pancreas.

ACKNOWLEDGMENTS

The authors thank Dr. Walter F. Boron for generously providing the NBC antibodies for this study (supported by DK30344). M.F.R. is supported by a Cystic Fibrosis Core Center grant (P30-DK27651). Research in F.T.'s laboratory is supported by a grant from the Deutsche Forschungsgemeinschaft (Th 345/6-1).

REFERENCES

1. Case, R. M., and Argent, B. E. (1989) *in Handbook of Physiology. The Gastrointestinal System* (Schultz, S. G., Forte, J. G., and Fauner, B. B., Eds.), Vol. 3, pp. 383–417, Oxford Univ., New York.
2. Sewell, W. A., and Young, J. A. (1975) *J. Physiol.* **252**, 379–396.
3. Seow, K. T., Lingard, J. M., and Young, J. A. (1986) *Am. J. Physiol.* **250**, G140–G148.
4. Cook, D. I., and Young, J. A. (1996) *in Comprehensive Human Physiology*. (Greger, R., and Windhorst, U., Eds.), Vol. 2, pp. 1327–1343 Springer, Berlin and Heidelberg, Germany.
5. Kasai, H., and Augustine, G. J. (1990) *Nature* **348**, 735–738.
6. Petersen, O. H. (1993) *in The Pancreas. Biology, Pathobiology, and Disease* (Go, V. L. W., DiMagno, E. P., Gardner, J. D., Lebenthal, E., Reber, H. A., and Scheele, G. A., Eds.), 2nd ed., pp. 191–218, Raven, New York.
7. Novak, I., and Greger, R. (1988) *Pflüger's Arch.* **411**, 546–553.
8. Novak, I., and Greger, R. (1988) *Pflüger's Arch.* **411**, 58–68.

9. Gray, M. A., Plant, S., and Argent, B. E. (1993) *Am. J. Physiol.* **264**, C591–C602.
10. Alper, S. L., Kopito, R. R., Libresco, S. M., and Lodish, H. F. (1988) *J. Biol. Chem.* **263**, 17092–17099.
11. Kopito, R. R., and Lodish, H. F. (1985) *Nature* **316**, 234–238.
12. Kopito, R. R., Lee, B. S., Simmons, D. M., Lindsey, A. E., Morgans, C. W., and Schneider, K. (1989) *Cell* **59**, 927–937.
13. Romero, M. F., and Boron, W. F. (1999) *Annu. Rev. Physiol.* **61**, 699–723.
14. Romero, M. F., Hediger, M. A., Boulpaep, E. L., and Boron, W. F. (1997) *Nature* **387**, 409–413.
15. Romero, M. F., Fong, P., Berger, U. V., Hediger, M. A., and Boron, W. F. (1998) *Am. J. Physiol.* **274**, F425–F432.
16. Abuladze, N., Lee, I., Newman, D., Hwang, J., Boorer, K., Pushkin, K., and Kurtz, I. (1998) *J. Biol. Chem.* **273**, 17689–17695.
17. Choi, I., Romero, M. F., Khandouri, N., Bril, A., and Boron, W. F. (1999) *Am. J. Physiol.* **276**, C576–C584.
18. Ishibashi, K., Sasaki, S., and Marumo, F. (1998) *Biochem. Biophys. Res. Commun.* **246**, 535–538.
19. Pushkin, A., Abuladze, N., Lee, I., Newman, D., Hwang, J., and Kurtz, I. (1999) *J. Biol. Chem.* **274**, 16569–16575.
20. Schmitt, B. M., Biemesderfer, D., Boulpaep, E. L., Romero, M. F., and Boron, W. F. (1999) *Am. J. Physiol.* **276**, F27–F38.
21. Thévenod, F., Dehlinger-Kremer, M., Kemmer, T. P., Christian, A. L., Potter, B. V. L., and Schultz, I. (1989) *J. Membr. Biol.* **109**, 173–186.
22. Thévenod, F., Hildebrandt, J. P., Striessnig, J., DeJonge, H. R., and Schultz, I. (1996) *J. Biol. Chem.* **271**, 3300–3305.
23. McLean, I. W., and Nakane, P. F. (1974) *J. Histochem. Cytochem.* **22**, 1077–1083.
24. Alper, S. L., Stuart-Tilley, A. K., Biemesderfer, D., Shmukler, B. E., and Brown, D. (1997) *Am. J. Physiol.* **273**, F601–F614.
25. Brown, D., Lydon, J., McLaughlin, M., Stuart-Tilley, A., Tyszkowski, R., and Alper, S. L. (1996) *Histochem. Cell Biol.* **105**, 261–267.
26. Burnham, C. E., Amlal, H., Wang, Z., Shull, G. E., and Soleimani, M. (1997) *J. Biol. Chem.* **272**, 19111–19114.
27. Romero, M. F., Sussman, C. R., Choi, I., Hediger, M. A., and Boron, W. F. (1998) *J. Am. Soc. Nephrol.* **9**, 11A. [abstract]
28. Muallem, S., and Loessberg, P. A. (1990) *J. Biol. Chem.* **265**, 12806–12812.
29. Muallem, S., and Loessberg, P. A. (1990) *J. Biol. Chem.* **265**, 12813–12819.
30. Boron, W. F., and Boulpaep, E. L. (1989) *Kidney Int.* **36**, 392–402.
31. Alper, S. L., Natale, J., Gluck, S., Lodish, H. F., and Brown, D. (1989) *Proc. Natl. Acad. Sci. USA* **86**, 5429–5433.
32. Brown, D., Hirsch, S., and Gluck, S. (1988) *Nature* **331**, 622–624.
33. Roussa, E., and Thévenod, F. (1998) *Eur. J. Morphol.* **36**(Suppl.), 147–152.
34. Roussa, E., Thévenod, F., Sabolic, I., Herak-Kramberger, C. M., Nastainczyk, W., Bock, R., and Schultz, I. (1998) *J. Histochem. Cytochem.* **46**, 91–100.
35. de Ondarza, J., and Hootman, S. R. (1997) *Am. J. Physiol.* **272**, G124–G134.
36. Villanger, O., Veel, T., and Raeder, M. G. (1995) *Gastroenterology* **108**, 850–859.
37. Zhao, H., Star, R. A., and Muallem, S. (1994) *J. Gen. Physiol.* **104**, 57–85.
38. Ishiguro, H., Steward, M. C., Lindsay, A. R., and Case, R. M. (1996) *J. Physiol.* **495**, 169–178.
39. Shumaker, H., Amlal, H., Frizzell, R., Ulrich, C. D., II, and Soleimani, M. (1999) *Am. J. Physiol.* **276**, C16–C25.